

Workspace and Force-Moment Transmission of a Variable Arm Type Parallel Manipulator

Se-Han Lee, Jae-Bok Song, Woo Chun Choi, Daehie Hong

Department of Mechanical Engineering, Korea University
5, Anam-dong Sungbuk-gu, Seoul, 136-701, Korea.

E-mail: jbsong@korea.ac.kr

Abstract

Kinematic and dynamic characteristics of Stewart platform based parallel manipulators are fixed once they are constructed. Thus parallel manipulators with various configurations are required to meet a variety of applications. In this research a variable arm type parallel manipulator (VAPM) has been developed, in which the length of the arm linking the platform center to the platform-leg contact point can be varied by the actuator. Workspace of the VAPM is larger than that of a traditional Stewart platform and especially the range in which the maximum orientation angles can be maintained is significantly expanded. Furthermore, the characteristics of force and moment transmission between the legs and platform can be adjusted to meet the requirements of various tasks. Kinematic and dynamics analysis was performed to verify the usefulness of the VAPM and the actual hardware was built to demonstrate the feasibility.

1. Introduction

Parallel manipulators such as a Stewart Platform [1] has some advantages of high rigidity, high accuracy, and high load-carrying capacity over serial manipulators. These manipulators have found a variety of applications in flight and vehicle simulators, high-precision machining centers, mining machines [2], motion simulator [3], and so on.

In the past decade, a significant amount of research has been done on developing the parallel manipulators with new configurations. Among them, Delta [4] and Hexaglide [5] mechanisms could perform rapid platform motion by moving heavy actuating parts toward the fixed base, and the hybrid manipulator [6] combined a 3-DOF serial mechanism with a 3-DOF parallel one. And Lee constructed the double parallel manipulator [7] in which parallel mechanisms were connected to improve stiffness and Stoughton [8] modified arrangement and structure of the actuators to improve performance of a conventional Stewart Platform. On the other hand, Arai [9] showed that the conventional Stewart Platform did not have an optimal configuration and suggested the new configuration.

In this research the new mechanism named a variable arm type parallel manipulator (VAPM) has been developed, in which the length of the arms linking the platform center to the platform-leg connection points can be varied by the actuator. By varying the arm lengths, workspace of the VAPM becomes changeable and

especially the range in which the maximum orientation angles can be maintained is significantly expanded. In addition, the Jacobian matrix of the VAPM can be changed by varying the arm lengths, thus leading to modification of the characteristics of force and moment transmission between the legs and platform center. This feature enables the VAPM to meet the requirements of various tasks.

The remainder of this paper is organized as follows. Chapter 2 presents the structure of the variable arm type parallel manipulator and the operational principle of the variable arm mechanism. Chapter 3 is concerned with the kinematic analysis and workspace analysis of the VAPM, and Chapter 4 deals with the force-moment transmission characteristics of the VAPM. Finally, conclusions are drawn in Chapter 5.

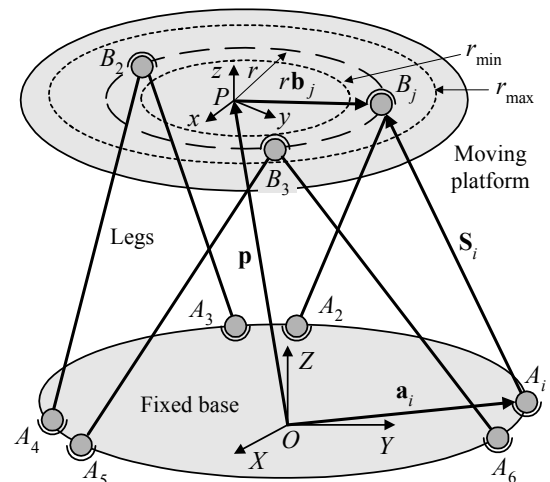


Fig. 1 Schematic of VAPM.

2. Variable Arm Type Parallel Manipulator

In this research a variable arm type parallel manipulator (VAPM) based on a Stewart platform is proposed. A Stewart platform shown in Fig. 1 consists of a moving platform, a fixed base, and six actuating legs, which connect the platform to the base. Characteristics of the parallel manipulator such as workspace and force/moment acting on the platform are affected by the connection position of the platform-leg and the base-leg. If these positions can vary, therefore, configuration of a parallel manipulator can be adjusted for the task requirements. Varying the position of the base-leg connection point, however, may cause stability problem and require a large

force for movement of the whole platform and legs. Hence the VAPM adopts variation of the position of platform-leg connection point.

2.1 Structure of VAPM

Figure 1 shows the variable arm type parallel manipulator whose appearance is similar to the conventional Stewart platform. The moving part of the leg is connected to the platform through a spherical joint. The connection point B_j ($j = 1, 2, 3$) is fixed in the conventional Stewart platform, while the connection point can be varied by the special actuating mechanism in the proposed VAPM.

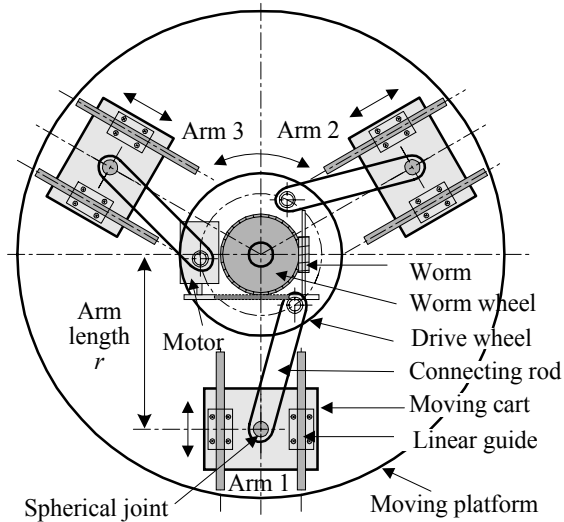


Fig. 2. Structure of variable arm mechanism.

Figure 2 illustrates the detailed structure of the actuating mechanism of the VAPM and Fig. 3 shows the photo of the constructed VAPM. The variable arm mechanism consists of 3 fictitious arms, which connect the platform center to the platform-leg connection point B_j . This mechanism is capable of varying the arm length in the range of the minimum arm length r_{\min} to the maximum arm length r_{\max} . Note that the mechanism is designed so that the 3 arms related to B_1, B_2, B_3 have the same length at all times. It is also noted that the configuration with the maximum arm length corresponds to the fixed type Stewart platform.

The platform-leg connection parts are mounted on the sliding carts, which move linearly on the linear guides arranged radially on the bottom of the platform. Rotation of the worm connected to the motor through the timing belt causes the worm wheel and thus the drive wheel rigidly linked to the worm wheel to rotate. This rotation of the drive wheel enables the 3 connecting rods to move the sliding carts continuously on the linear guides.

The variable arm mechanism employs the worm gear in which only the worm is able to drive the worm wheel, and

not vice versa. That is, any force acting on the connection parts cannot rotate the motor in reverse through the worm gear. This feature provides a kind of locking mechanism, which is of great importance to safety of the VAPM.

Physical dimensions of the constructed VAPM are indicated in Fig. 4. As shown in the figure, the arm length can be adjusted in the range between 0.16m and 0.32m. And the maximum and minimum lengths of the leg are $L_{\min} = 0.735\text{m}$ and $L_{\max} = 0.985\text{m}$, respectively.

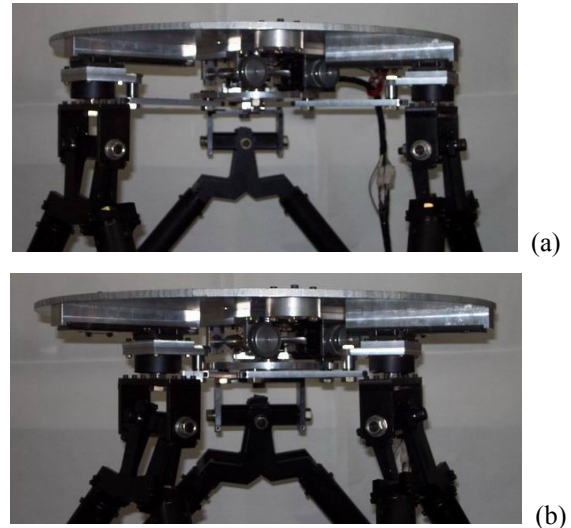


Fig. 3 Photos of variable arm type parallel manipulator: (a) maximum arm length, and (b) minimum arm length.

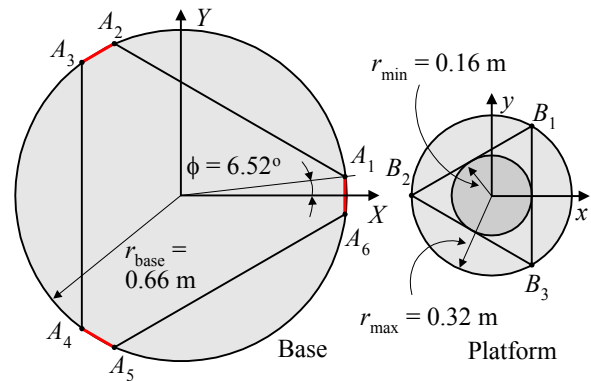


Fig. 4 Physical dimensions of fixed base and platform.

3. Characteristics of VAPM

The VAPM may be classified into the redundant manipulator since it has an extra degree of freedom provided by the actuating mechanism for the variable arm. In most cases, however, the arm length is adjusted not on a real-time basis during the task, but off-line before the task according to the specific requirements. The number of degrees of freedom, therefore, is still six. Hence kinematic and dynamic equations for the conventional

parallel manipulators are applicable to the VAPM. If the arm length is desired to vary on a real-time basis, new analysis for 7 DOFs will be needed.

3.1 Kinematics of VAPM

In this section the kinematic analysis of both the variable arm mechanism and the VAPM is briefly discussed. The moving platform frame xyz and the fixed reference frame XYZ are attached to the platform center and the base center, respectively, as shown in Fig. 1. The platform orientation is described by the following Z-Y-X Euler angles. First, the platform frame xyz is rotated about the z -axis by α , then rotated about the current y -axis by β , and then rotated about the current x -axis by γ .

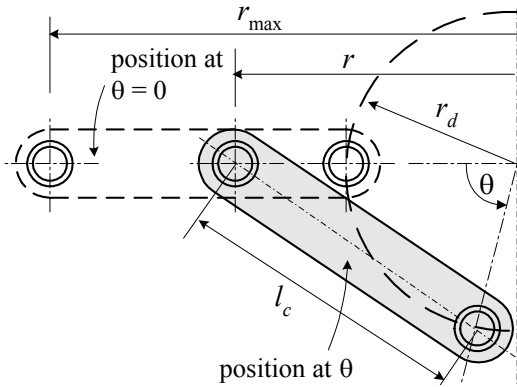


Fig. 5 Geometry of variable arm.

Figure 5 illustrates the change in the connecting rod according to the drive angle θ , which is the rotation angle of the drive wheel of the variable arm mechanism. The relationship between the connecting rod length l_c , drive wheel radius r_d , and the drive angle θ is given by

$$l_c^2 = r^2 + r_d^2 - 2rr_d \cos\theta \quad (1)$$

On the other hand, the position of the platform-leg connection point B_j is described by

$$\mathbf{a}_i + \mathbf{S}_i = \mathbf{p} + r\mathbf{R}\mathbf{b}_j, \quad i = 1, \dots, 6 \quad (2)$$

$(j = 1 \text{ for } i = 1, 2, j = 2 \text{ for } i = 3, 4, j = 3 \text{ for } i = 5, 6)$

where \mathbf{R} is the rotation matrix to describe rotation of the platform frame xyz relative to the reference frame XYZ . It is noted that both sides of Eq. (2) represent the position vector from the origin of the reference frame XYZ to the connection point B_j . Since the vector \mathbf{b}_j is the unit vector in the platform frame, pre-multiplication of \mathbf{R} in $\mathbf{R}\mathbf{b}_j$ makes it expressed relative to the reference frame. Eq. (2), composed of 6 equations, is the basic equation to represent the kinematic constraints of the VAPM.

The inverse kinematic problem where the leg lengths are determined for a given platform position/orientation can be expressed by

$$\mathbf{S}_i = \mathbf{p} + r\mathbf{R}\mathbf{b}_j - \mathbf{a}_i \quad (3)$$

Since the vector can be represented by $\mathbf{S}_i = L_i \mathbf{s}_i$, where L_i denotes the leg length and \mathbf{s}_i is the unit vector from A_i to B_j , the leg length is obtained by

$$L_i = \|\mathbf{S}_i\| = \|\mathbf{p} + r\mathbf{R}\mathbf{b}_j - \mathbf{a}_i\| \quad (4)$$

Note that the leg length can be uniquely determined for the given position vector \mathbf{p} and rotation matrix \mathbf{R} .

The direct kinematic problem where the platform position/orientation is computed for the given leg lengths can be solved by

$$L_i \mathbf{s}_i - \mathbf{p} - r\mathbf{R}\mathbf{b}_j + \mathbf{a}_i = 0 \quad (i = 1, \dots, 6) \quad (5)$$

Since the six equations of Eq. (5) are coupled to each other and in the form of implicit functions, the multiple solutions may exist [10], and the solutions can be obtained by numerical analysis except for the special cases [11].

3.2 Workspace analysis for VAPM

Workspace is the space which the platform can reach in the task space. In conventional parallel manipulators, their workspace is fixed, once they are constructed. As mentioned before, the VAPM is capable of varying the workspace by changing its configuration at any time.

First, the translation workspace with the platform orientation fixed at $\alpha = \beta = \gamma = 0^\circ$ is investigated. Figures 6 and 7 show the boundaries of the maximum range in which the platform center can reach in the XZ and YZ planes when the VAPM are at the maximum and minimum arm lengths, respectively (i.e., $r = r_{\max}$ and $r = r_{\min}$). It is observed that there is little difference in translation workspace for these two cases.

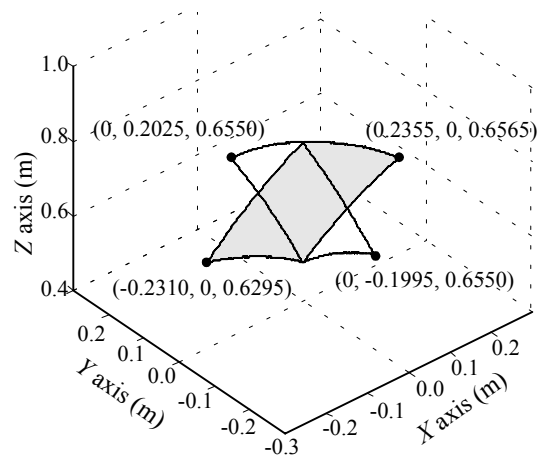


Fig. 6 Translation workspace for maximum arm length.

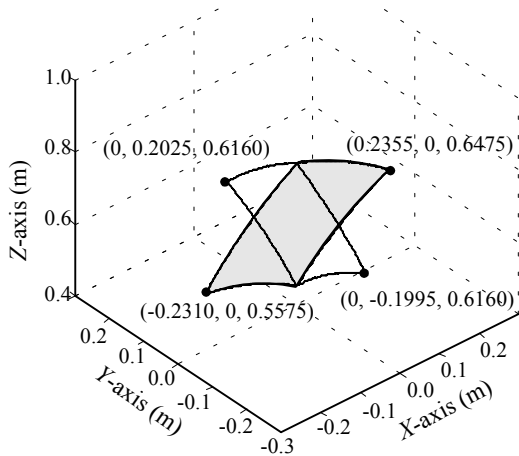


Fig. 7 Translation workspace for minimum arm length.

Figure 8 shows the maximum reachable range for each axis as the arm length continuously varies from $r = r_{\min}$ to $r = r_{\max}$. In the X and Y axes, little change in the maximum reachable range is observed. In the Z axis, the maximum reachable range tends to reduce as the arm length decreases, but the maximum stroke, the difference between the maximum reachable distances in the directions of $+Z$ and $-Z$ axes, slightly increases from 0.323m to 0.344m as the arm length decreases.

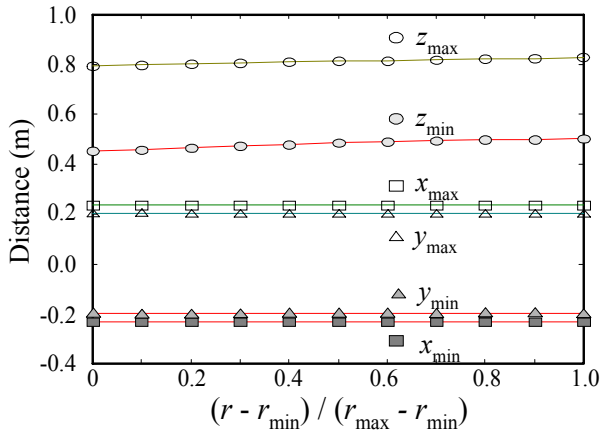


Fig. 8 Changes in translation workspace for continuously varying arm length.

Next, the orientation workspace will be investigated. Figures 9 and 10 show the maximum reachable orientation angles α , β , γ as the platform moves along the Z -axis for the maximum and minimum arm lengths. Referring to Fig. 9, the orientation angle α about the Z -axis for the maximum arm length becomes maximum ($\alpha = 38.4^\circ$) at $Z = 0.65\text{m}$, and the maximum orientation angles for β , γ are slightly smaller than that for α . However, the orientation angles for α , β , γ for the

minimum arm length have the maximum of 58.8° , which is about 1.5 times larger than those for the maximum arm length. In addition, the angle α can maintain the maximum angle in the range of $Z = 0.55$ to 0.65m , which is much larger than the case of the maximum arm length. This large range holds for β and γ , although it is slightly smaller than that for α .

In summary, the VAPM can provide larger workspace than the fixed type parallel manipulator, and the maximum orientation angles can be achieved over the wide range of motion. This feature of VAPM shows possibility of different applications with the single mechanism. For example, it can be used for both the flight simulator that requires large rotational motion and the vehicle simulator in which small rotational motion is sufficient.

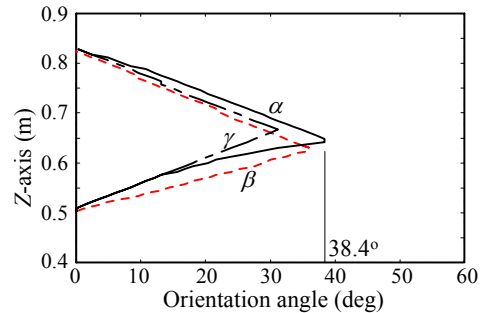


Fig. 9 Orientation workspace for maximum arm length.

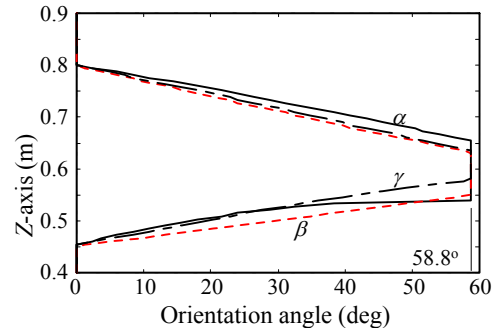


Fig. 10 Orientation workspace for minimum arm length.

4. Force-Moment Transmission of VAPM

The relationship between the velocity of the leg actuator and the velocity of the platform center is given by

$$\mathbf{J} \dot{\mathbf{X}} = \dot{\mathbf{L}} \quad (7)$$

where $\dot{\mathbf{X}} = \{\mathbf{v}_P^T \ \boldsymbol{\omega}_P^T\}^T$ denotes the linear and angular velocities of the platform center, and $\dot{\mathbf{L}} = \{\dot{L}_1, \dots, \dot{L}_6\}^T$ is the linear velocity vector of the moving part of the leg, respectively. The Jacobian matrix in Eq. (7) can be expressed by

$$\mathbf{J} = \begin{bmatrix} \mathbf{s}_1 & \cdots & \mathbf{s}_6 \\ r(\mathbf{Rb}_1 \times \mathbf{s}_1) & \cdots & r(\mathbf{Rb}_3 \times \mathbf{s}_6) \end{bmatrix}^T \quad (8)$$

It is noted that the elements of the Jacobian matrix \mathbf{J} include the arm length r and thus the characteristics of \mathbf{J} can vary through adjustment of r .

On the other hand, the actuator force \mathbf{F}_L and platform force/moment \mathbf{F}_X has the following relation

$$\mathbf{F}_X = \mathbf{J}^T \mathbf{F}_L \quad (9)$$

\mathbf{F}_X can be partitioned into the force vector \mathbf{F} and moment vector \mathbf{M} as follows:

$$\begin{Bmatrix} \mathbf{F} \\ \mathbf{M} \end{Bmatrix} = \begin{Bmatrix} \mathbf{J}_f \\ \mathbf{J}_m \end{Bmatrix} \mathbf{F}_L \quad (10)$$

$$\mathbf{J}_f = [\mathbf{s}_1 \quad \cdots \quad \mathbf{s}_6] \quad (11a)$$

$$\mathbf{J}_m(r) = r[(\mathbf{Rb}_1 \times \mathbf{s}_1) \quad \cdots \quad (\mathbf{Rb}_3 \times \mathbf{s}_6)] \quad (11b)$$

Eq. (10) can be rewritten by

$$\mathbf{F} = \mathbf{J}_f \mathbf{F}_L, \quad \mathbf{M} = \mathbf{J}_m(r) \mathbf{F}_L \quad (12)$$

It is observed that the gain matrix \mathbf{J}_m between the actuator force vector and platform moment vector is a function of the arm length r . This means that a change in the arm length directly affects \mathbf{J}_m , but only has an indirect effect on \mathbf{J}_f by means of changes in the directions of the unit vectors $\mathbf{s}_1, \dots, \mathbf{s}_6$ due to a change in manipulator configuration caused by adjustment of the arm length.

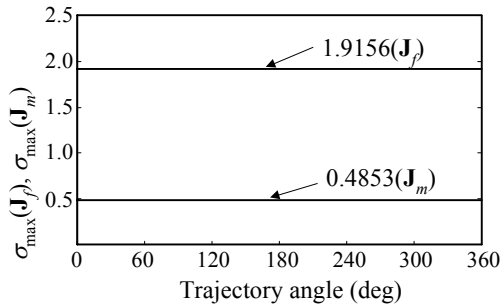


Fig. 11 Force-moment transmission gains for maximum arm length.

Figures 11 and 12 show the maximum singular values of \mathbf{J}_f and \mathbf{J}_m for the maximum and minimum arm lengths when the platform center is commanded to follow the circular trajectory with the radius of 0.1m. These maximum singular values $\sigma_{\max}(\mathbf{J}_f)$ and $\sigma_{\max}(\mathbf{J}_m)$ correspond to the maximum gain for force transmission (\mathbf{J}_f) and the maximum gain for moment transmission (\mathbf{J}_m), respectively. It is found that the change in $\sigma_{\max}(\mathbf{J}_f)$ is not large for the maximum arm length, but $\sigma_{\max}(\mathbf{J}_m)$ for the minimum arm length has increased 2.06 times compared

to that for the maximum arm length.

Figure 13 shows the maximum singular values as the arm length continuously varies from $r = r_{\min}$ to $r = r_{\max}$. It is observed that $\sigma_{\max}(\mathbf{J}_f)$ changes only slightly, but $\sigma_{\max}(\mathbf{J}_m)$ increases relatively rapidly with the arm length. In summary, the moment transmission gains can be doubled by varying the arm length.

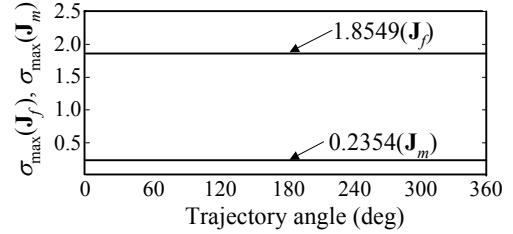


Fig. 12 Force-moment transmission gains for minimum arm length.

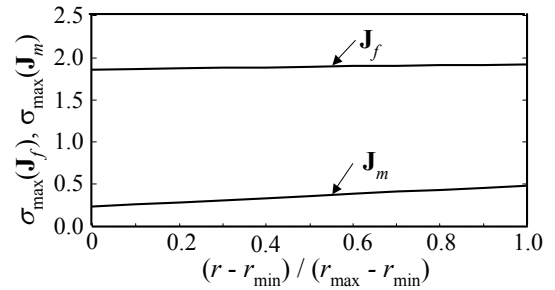


Fig. 13 Changes in force-moment transmission gains for continuously varying arm length.

Meanwhile, the Jacobian matrices \mathbf{J}_f and \mathbf{J}_m can provide the information on how isotropically the force and moment are generated. In general, the manipulator should generate force and moment as isotropically as possible at the platform. If sufficient force/moment cannot be produced in some direction compared with other directions, the efficient task may not be performed and sufficient stiffness may be provided in that direction.

The condition numbers C_f and C_m for the Jacobian matrices \mathbf{J}_f and \mathbf{J}_m are expressed by

$$C_f = \sigma_{\max}(\mathbf{J}_f) / \sigma_{\min}(\mathbf{J}_f) \quad (13a)$$

$$C_m = \sigma_{\max}(\mathbf{J}_m) / \sigma_{\min}(\mathbf{J}_m) \quad (13b)$$

The condition number is in the range of one to infinity. As the number approaches one, the force/moment are produced more isotropically, which is desirable in most cases. On the other hand, if the mechanism is in and around singular configurations, the condition number approaches infinity since the minimum singular value becomes zero or small.

Figures 14 and 15 illustrate the condition number profiles for the force and moment on the XY plane ($-0.1\text{m} \leq X \leq 0.1\text{m}$, $-0.1\text{m} \leq Y \leq 0.1\text{m}$) at the height $Z = 0.667\text{m}$. It is shown in Fig. 14 that the force condition number

decreases in the range of 4.8% to 7.6% as the arm length decreases, which means improved isotropy. As shown in Fig. 15, on the contrary, the moment condition number increases slightly as the arm length decreases.

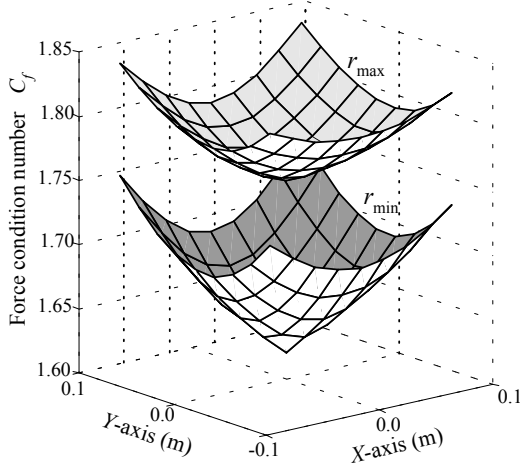


Fig. 14 Force condition number C_f at the maximum and minimum arm lengths on the XY plane.

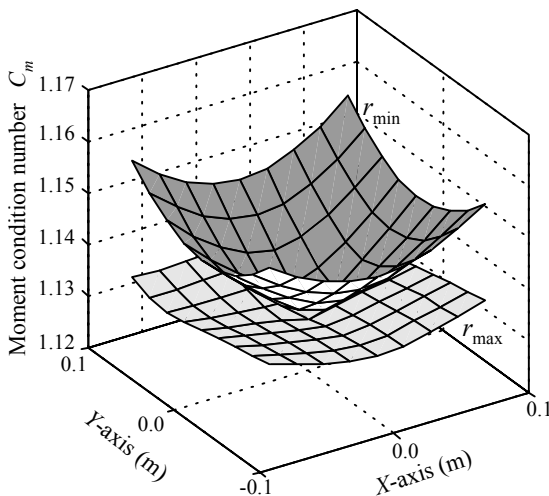


Fig. 15 Moment condition number C_m at the maximum and minimum arm lengths on the XY plane.

5. Conclusions

In this research the variable arm type parallel manipulator (VAPM) was developed based on the conventional Stewart platform. The VAPM capable of varying the configuration by adjustment of the platform-leg connection point can change the kinematic and dynamic characteristics of the parallel manipulator.

Orientation workspace can be increased more than 1.5 times compared to the conventional parallel manipulators. The motion range in which the maximum orientation

angles can be maintained has significantly increased. Varying the manipulator configuration causes the Jacobian matrix to be changed, and thus the moment transmission characteristics from the actuating leg to the platform center can be adjusted according to the types of tasks.

Acknowledgements

This research was supported by the Basic Research Program of the Korea Science and Engineering Foundation (1999-1-304-003).

References

- [1] D. Stewart, A platform with six degrees of freedom, *Proc. of Inst. Mech. Engr.*, Vol. 180, No. 1, pp. 371 – 386, 1965.
- [2] K. Nakashima, etc., Development of the parallel manipulator, *Robotics, Mechatronics and Manufacturing systems*, Elsevier Science Pub., pp.27-32., 1993.
- [3] N. Mimura, and Y. Funahashi, A new analytical system applying 6 DOF parallel link manipulator for evaluating motion sensation, *Proc. of ICRA 1995*, pp.227-233., 1995.
- [4] F. Pierrot, A. Fournier, P. Dauchez, Towards a fully parallel 6-dof robot for high speed applications, *Proc. of ICRA*, pp.1288-1293, 1991.
- [5] M. Honegger, A. Codourey, E. Burdet, Adaptive control of the Hexaglide, a 6-dof parallel manipulator, *Proc. of ICRA 1997*, pp.543-548, 1997.
- [6] K. J. Waldron, M. Raghavan, B. Roth, Kinematics of a hybrid series-parallel manipulation system, *ASME Journal of Dynamic Systems, Measurement, and Control*, Vol. 111, pp. 211-221, 1989.
- [7] M. K. Lee, Design of a high stiffness machining robot arm using double parallel mechanisms, *Proc. of ICRA 1995*, pp.234-240, 1995.
- [8] R. S. Stoughton, T. Arai, A modified Stewart platform manipulator with improved dexterity, *IEEE Transactions on Robotics and Automation*, Vol. 9, No. 2, pp. 166-173, 1993.
- [9] T. Arai, K. Cleary, T. Nakamura, H. Adachi, K. Homma, Design, analysis and construction of a prototype parallel link manipulator, *Proc. of IROS 1990*, pp. 205-212, 1990.
- [10] M. Raghavan, The Stewart platform of general geometry has 40 configurations, *Journal of Mechanical Design*, pp. 277-280, 1993.
- [11] E-M. Dafaoui, Y. Amirat, J. Pontnau, C. Francois, Analysis and design of a six-dof parallel manipulator; modeling, singular configurations and workspace, *IEEE transactions on Robotics and Automation*, Vol. 14, No.1, pp.78-92, 1998.